A Simple and Scalable Model for Spiral Inductors on Silicon

C. B. Sia[1], K. S. Yeo[1], W. L. Goh[1], T. N. Swe[1], J. G. Ma[1], M. A. Do[1], J. S. Lin[2] and L. Chan[3]

[1] School of Electrical and Electronic Engineering,
Nanyang Technological University, Singapore 639798, p7435887z@ntu.edu.sg
[2] Bell Laboratories, 600 Mountain Avenue, Murray Hill, NJ 07974, USA
[3] Chartered Semiconductor Manufacturing Ltd,
60 Woodlands Industrial Park D Street 2, Singapore 738406

ABSTRACT

A new, simple and scalable inductor model for silicon-based spiral inductors has been presented in this paper. Compared to the conventional model, it can predict accurately the inductive characteristics and quality factor for inductors of different sizes. Introduction of a physical, non-frequency dependent resistive element to model conductor skin effects offers simplicity and accuracy to the modeling process of planar spiral inductors.

Keywords: Spiral inductor, physical model, inductance, quality factor and skin effect.

1 INTRODUCTION

Increasing demands for personal mobile communication equipment has motivated surging research interest to focus on the development of inexpensive, small size, low power consumption and low noise level systems [1]. Silicon, with its mature technology, low fabrication cost as well as high packing density is recognized as the only suitable material able to satisfy the needs of this rapidly growing communication market [2]. To fulfill all the above-mentioned requirements, one of the most important and indispensable circuit components is the on-chip silicon-based spiral inductor.

Over the past few years, many researchers have put in enormous efforts but achieving high performance inductors on silicon still remains a great challenge. The current CMOS process uses a very conductive silicon substrate. Spiral inductors fabricated on such lossy substrate suffer from undesirable energy dissipation in terms of capacitive and magnetic losses [3,4]. In addition, high resistive loss of aluminum metal lines at GHz frequency range further degrades the performance of silicon-based inductors.

To exploit full capabilities offered by such monolithic inductors, the limitations imposed by the silicon technology must be accurately modeled and characterized. Conventional techniques used to model such inductors usually adopt numerical methods or parameter fitting. Such models are generally not scalable over a wide range of layout and process conditions. A simple, accurate, physical and scalable inductor model is an essential tool for both RF IC designers and process engineers. It not only serves to predict the inductor's behavior for future technologies, but also proves to be very instrumental in developing guidelines for achieving the optimal inductor design.

2 RC PARASITICS OF SPIRAL INDUCTORS

Accurate and physical modeling of silicon-based inductors fundamentally requires identification of all the relevant parasitics present in the inductor's structure and comprehensive understanding of their effects. The inductor is design primarily for storing magnetic energy. All ohmic and capacitive parasitics present in a silicon-based inductor are counter-productive. As such, these parasitics must be modeled carefully so that the overall inductor behavior can be accurately depicted. In this paper, a new physical and scalable inductor model is presented.

Figure 1 compares the new inductor model to the physical model reported in [5]. The two models consist of principally the main series branch, L_s, R_s and C_s. L_s represents the conductor's lumped series inductance; R_s characterizes the metallization series resistance as well as skin depth of the conductor; C_s denotes the dielectric capacitance between the spiral and center-tap underpass; C_{ox} models the oxide parasitic capacitance between the spiral and substrate; and finally C_{si} and R_{si} provide a representation of the lossy silicon substrate underneath the inductor.

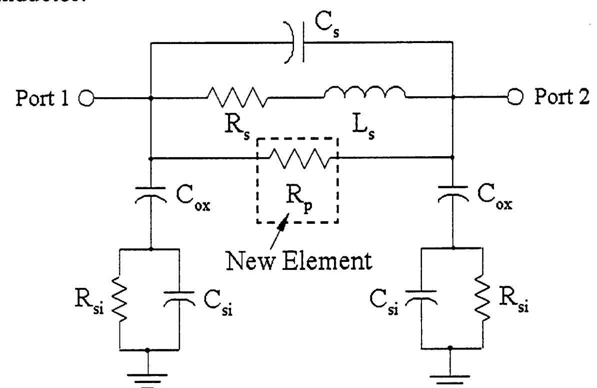

Figure 1: New Model for Silicon-based Spiral Inductor.

The top and cross-sectional views of a silicon-based conventional square spiral inductor are shown in Figure 2. It identifies all individual resistive and capacitive parasitic components present in the structure of a real spiral inductor.

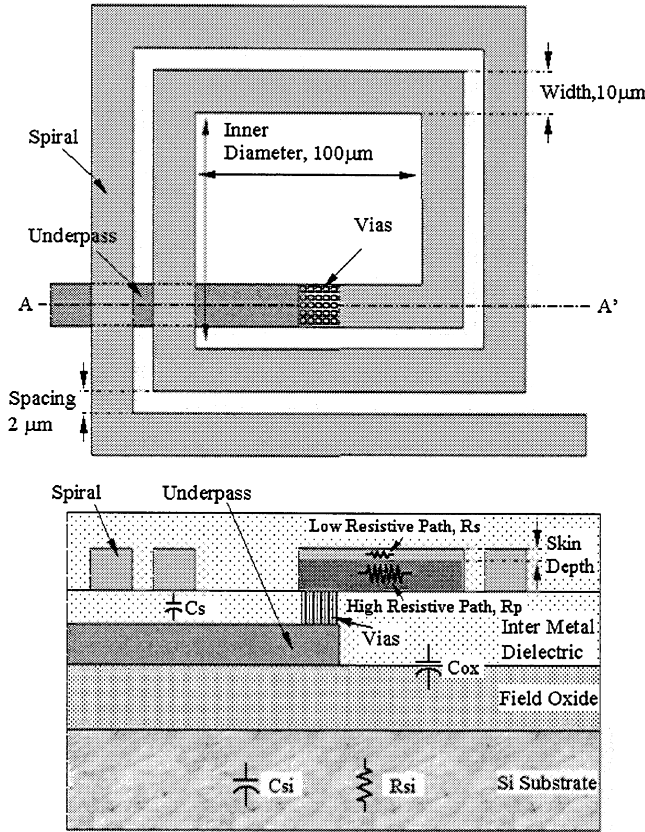

Figure 2: Layout of Conventional Square Spiral Inductor.

L_s, the series inductance of spiral inductor is evaluated using Greenhouse algorithm for computing inductance of planar rectangular spiral inductor [6]. In the literature, many empirical formulae have already been developed to estimate the spiral inductance. Nonetheless, the Greenhouse technique offers the most accurate results. This method basically determines the overall inductance of a spiral by summing the self inductance of each wire segments as well as the positive and negative mutual inductances between all wire pairs.

In [5], series resistance R_s of the whole spiral metal conductor is formulated taking into consideration its resistance at dc as well as high frequencies. As frequency increases, the current density within the metal conductor becomes non-uniform. This is due to the formation of eddy currents when the conductor is subjected to a time-varying magnetic field. Such eddy currents reduce the net current flow within the conductor and hence cause an increase in the ac resistance. Therefore, the final expression used to describe the series resistance R_s is a function of frequency. R_s is expressed as

$$R_s = \frac{\rho \cdot l}{w \cdot t_{eff}}; \quad (1)$$

where $t_{eff} = \delta \cdot (1 - e^{-t/\delta})$ and $\delta = \sqrt{\frac{\rho}{\pi \mu f}}$

In the above expressions, ρ, l, w and t correspond to the resistivity, length, width and thickness of the metal conductor respectively. t_{eff} refers to the effective conductor thickness at high frequencies. δ and μ are the skin depth and permeability of the metal conductor respectively.

As compared to the conventional model, our new proposed model has 2 resistive elements to predict the resistive behavior of the metal conductor at all frequencies. A new resistive element R_p has been introduced to model the skin effects as well as non-uniform current flow within the metal conductor. This new resistive parasitic basically describes the high resistive path within the metal conductor when the inductor operates in the high frequencies.

On the other hand, parasitic capacitance, C_s describes the capacitive coupling between input and output ports of the inductor. From Figure 2, we can observed that there are actually coupling capacitances between the underpass and spiral as well as within the different turns of spiral itself, between adjacent turns of the metal conductor. The overlap capacitance is more significant since there is a larger potential difference between the spiral and the underpass [5]. As such, modeling C_s with only the sum of all overlap capacitances is sufficiently accurate.

$$C_s = N \cdot w^2 \cdot \frac{\varepsilon_{oxide}}{t_{oxide1}} \quad (2)$$

Where N is the number of overlap; w is the width of the spiral; t_{oxide1} is the oxide thickness between the spiral and underpass.

C_{ox}, C_{si} and R_{si} represent the lossy substrate underneath the inductor. C_{ox} describes the oxide capacitance between the spiral and the substrate. C_{si} and R_{si} on the other hand, predict the undesirable substrate energy dissipation of the inductor especially at high frequencies. These parasitics are proportional to the area occupied by the inductor and can be calculated using

$$C_{ox} = \frac{1}{2} \cdot l \cdot w \cdot \frac{\varepsilon_{oxide}}{t_{oxide2}} \quad (3)$$

$$C_{si} = \frac{1}{2} \cdot l \cdot w \cdot C_{substrate} \quad (4)$$

$$R_{si} = \frac{2}{l \cdot w \cdot G_{substrate}} \quad (5)$$

Where t_{oxide2} is the oxide thickness between the spiral and the substrate, $C_{substrate}$ and $G_{substrate}$ are the per unit area conductance and capacitance of the substrate.

3 EXPERIMENTAL RESULTS

To test the scalability of our new model, three conventional square spiral inductors with 4, 6 and 8 turns, having physical dimensions shown in Figure 2 are fabricated on the 0.25μm technology to obtain the experimental data. Table 1 tabulates the physical parameters for the inductor's design dimensions and fabrication process. Table 2 consolidates the calculated and simulated values of all model elements for the 3 inductors.

Physical Parameters:	
Metal Width	: 10 μm
Metal Thickness	: 1.5 μm
Spacing	: 2 μm
Inner Diameter	: 100 μm
Oxide Thickness (C_{ox})	: 4.5 μm
Oxide Thickness between Spiral & Underpass	: 1.3 μm
Resistivity of Si	: 50 Ωcm
Resistivity of Al	: 3×10^{-6} Ωcm

Table 1: Physical Parameters for the Inductor's Design Dimensions and Fabrication Process.

No. of Turns	4 (3nH)	6 (5nH)	8 (10nH)
L_s (nH)	2.77	4.63	9.55
R_s (Ω)	4.67	8.16	12.41
C_s (fF)	10.63	15.93	21.24
C_{ox} (fF)	179.17	312.94	476.16
R_{si} (kΩ)	13.38	7.66	5.03
C_{si} (fF)	52.1	70.5	92.4
R_p (kΩ)	1.256	2.232	3.405
ρ_{Rp} (Ωcm)	8.01E-04	8.21E-04	8.23E-04

Table 2: Calculated Model Components for the 3 Inductors.

The three inductors are first modeled by adopting the technique outlined in [5], whereby R_s is solved as a function of skin depth and frequency shown in Equation (1). In this equation, it is assumed that beyond the conductor's skin depth, there is no current flow. From Figures 3, 4 and 5, the inductance plots for this conventional model matches closely to the measured data. Quality factor prediction using the conventional model for the 3 inductors is, however, fairly inaccurate. And when the inductor gets larger, accuracy of the conventional model start degrading significantly.

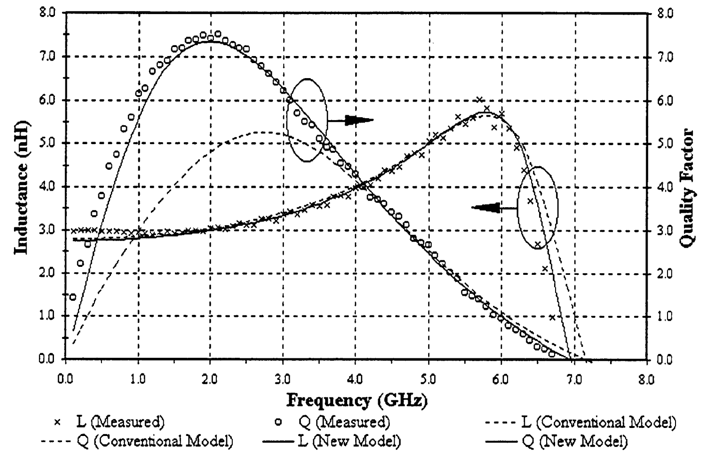

Figure 3: Inductance and Quality Factor Plot for 4-Turn Inductor.

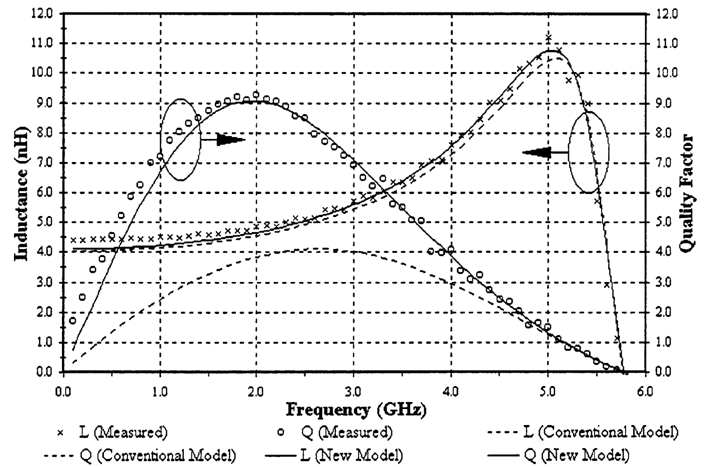

Figure 4: Inductance and Quality Factor Plot for 6-Turn Inductor.

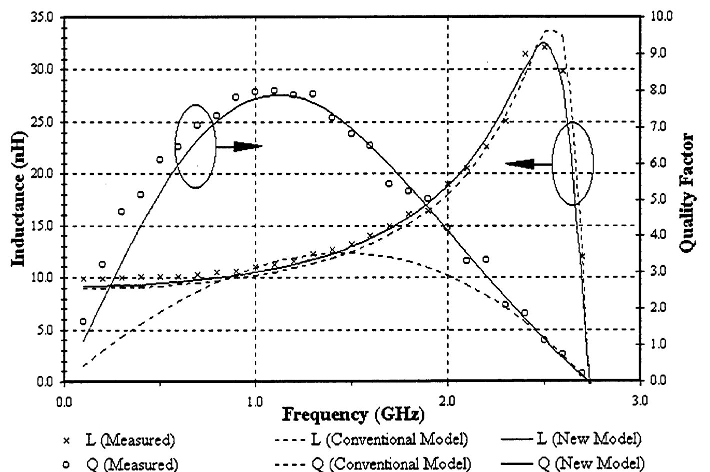

Figure 5: Inductance and Quality Factor Plot for 8-Turn Inductor.

As mentioned earlier in Section 2, our new model has an additional element, R_p, to describe skin effects as well as non-uniform current flow within the conductor. Beyond the conductor's skin depth is actually a very high resistive path, with little current flowing. It can therefore be modeled as a resistor in parallel with the main series branch. Figures 3, 4 and 5 show that this new model is able to predict accurately both the inductance and quality factor behavior for all 3 inductors from dc up to their resonant frequencies.

The values of R_s used for the 3 inductors are their respective conductor resistance at dc. R_p has been optimized to achieve good fit of the inductance as well as quality factor plots for the 3 inductors. Nevertheless, this new element has been shown to be scalable and physical since it has a constant resistivity of about 270 times more than ρ_{AL} at dc for all the 3 cases of different conductor lengths (See Table 2).

This new frequency independent element R_p simplifies the whole modeling process of the silicon-based spiral inductors reducing the model's complexity of having frequency dependent elements. Therefore, with the development of this simple, physical and scalable model, accurate predictions can be made and design guidelines can be developed for achieving high performance inductors. (See Figure 6)

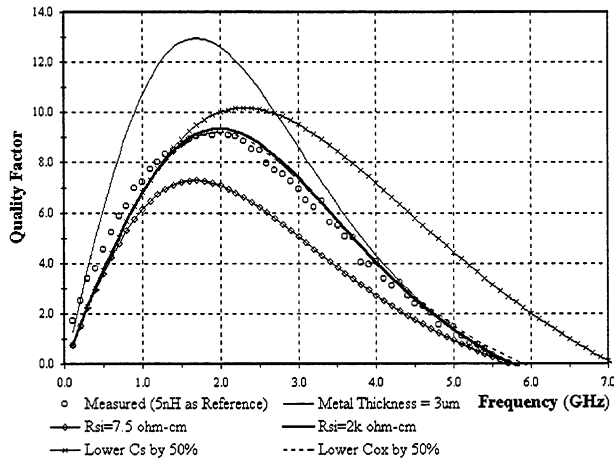

Figure 6: Effects of Parasitics on Inductor's Quality Factor.

4 CONCLUSIONS

A new inductor model for silicon-based spiral inductors has been presented in this paper. Compared to the conventional model, it is able to accurately predict both the inductive characteristics as well as quality factor for inductors with different number of turns. The introduction of a physical, non-frequency dependent resistive element to model the skin effects and non-uniform current flow not only simplifies the modeling process of planar spiral inductors but also offers much better accuracy.

REFERENCES

[1] P. R. Gray and R. G. Meyer, "Future directions in silicon IC's for RF personal communications," Proc. IEEE 1995 Custom Integrated Circuit Conf., pp. 83-90, May 1995.

[2] N. Camilleri, D. Lovelace, J. Costa, and N. David, "New development trends for silicon RF device technologies," IEEE Microwave and Millimeter-Wave Monolithic Circuits Symp., pp. 5-8, June 1994.

[3] C. P. Yue, C. Ryu, J. Lau, T. H. Lee, and S. S. Wong, "A physical model for planar spiral inductors on silicon," IEDM Tech. Dig., pp. 155-158, Dec 1996.

[4] J. Craninckx, and M. S. J. Steyaert, "A 1.8-GHz low-phase-noise CMOS VCO using optimized hollow spiral inductors," IEEE J. Solid-State Circuits, vol. 32, pp. 736-744, May 1997.

[5] C. Patrick Yue and S. Simon Wong, "Physical modeling of spiral inductors on silicon," IEEE Trans. Electron Devices, vol. 47, no.3, pp. 560-568, Mar 2000.

[6] H. M. Greenhouse, "Design of planar rectangular microelectronic inductors," IEEE Trans. Parts, Hybrids, Pack., vol. PHP-10, pp. 101-109, June 1974.